PAPER

Check for updates

Stability and transformation products of rubber derived compounds under various storage conditions

Phillip Berger, ID ab Katherine Poisson,ab Jaime Adams ID ac and Zhenyu Tian ID *abc

Rubber derived compounds (RDCs) are a growing environmental concern. Several chemical classes of RDCs are known for their transformation potential, making the quantification of these compounds in samples difficult if not run directly after sampling. We performed a targeted stability study with 23 standards in a mixture of 31 rubber derived compounds placed under different solvent conditions at three temperature points in order to gauge the long-term stability of the compounds under various storage conditions. Methanol at −20 °C was found to be the best solvent for storage, while acidified DI water was the least stable. Our study indicates that the addition of glutathione at or below 12.3 μg mL^{-1} does not prevent transformation of PPDs at relevant concentrations. Six compounds that showed loss during the targeted study were investigated using high resolution mass spectrometry to determine what transformations were occurring. Transformations for 2,2,4-trimethyl-2,4-hydroquinoline primarily formed 2,4-dimethylquinoline while 4-ADPA, 4sDPA, and HMMM involved a breakdown of the parent compound. Interestingly, MBT showed negligible loss indicating that the previous degradation was due to inter-compound interactions rather than the solvent they are stored in. Finally, the 31 standard mix was investigated using high resolution mass spectrometry with 91 unique features identified whose formations likely originate from reactions between RDCs. These results showcase the degradation and transformations that can occur for samples awaiting analysis under various storage conditions.

Environmental significance

Transformation products of organic contaminants are a growing concern, with the potential for the products to be more toxic than the parent compounds. Rubber derived compounds are a group of chemicals that highlight this issue with 6PPD-Q, a transformation product of 6PPD, being acutely toxic to coho salmon. Our study examines the stability of rubber derived compounds under 15 different storage conditions, and identifies transformation products that are formed during storage. The results will help reduce the number of false positives for environmental transformation products and increase confidence in quantitation of samples that were previously stored.

1 Introduction

With an estimated 82 million motor vehicles sold in 2024[1] worldwide, the number of tires in use expands yearly. While the exact composition of tires varies due to different brands and intended use of tires (passenger, commercial, and weather specific), tires are generally comprised of rubber and fillers,[2] with up to 12%[3,4] of the tire weight made up of additives. These additives include accelerants, antioxidants, antiozonants, and vulcanizers.[5] Over time, these additives migrate into the environment *via* tire wear particles,[6–16] with one study finding over 145 compounds with the capability to leach out of tires.[17] The most infamous of these compounds is 6PPD, an antiozonant added to tires to prevent ozone cracking.[5] When exposed to ozone it converts to the transformation product (TP) 6PPD-Q[18] which is acutely toxic to coho salmon in the Pacific Northwest. Tire leachates have been found to be toxic to multiple aquatic organisms[19–21] and biological assays[22–26] with further research beginning to narrow down the specific compounds that cause this toxicity.

Research has shown that many RDCs are inherently unstable.[27–30] Some of them are designed to protect rubber tires against environmental aging processes, such as oxidation,[18,31,32] hydrolysis,[33] and photolysis. However, this instability makes quantification of these compounds difficult, leading to speculation surrounding reports of RDC concentrations. Attempts have been made to stabilize these compounds by protecting

Department of Chemistry and Chemical Biology, College of Science, Northeastern University, Boston, MA, USA. E-mail: z.tian@northeastern.edu

Barnett Institute for Chemical and Biological Analysis, Northeastern University, Boston, MA, USA

Department of Marine and Environmental Sciences, Northeastern University, Boston, MA, USA

them with antioxidants,[34] such as glutathione. Other reports[35] indicate that at cold temperatures in a pH 2 medium, 6PPD is stable for up to four weeks. No study has yet explored and reported data on whether these conditions sufficiently protect PPDs from transformation, posing questions regarding the stability of the various compound classes that make up RDCs, and if one storage condition could benefit one class but negatively affect another. Furthermore, if RDCs transform into more stable products, future monitoring activities may focus on stable TPs rather than just the parent compounds.

To better understand how different storage conditions affect samples containing RDCs, we conducted a targeted study to observe the stability of 23 RDCs under 15 different storage conditions. These conditions were based on organic/aqueous solvents, temperature of storage, and the chemical properties of studied RDCs (e.g., amines and guanidines are sensitive to pH). We then conducted Non-Targeted Analysis (NTA) using high resolution mass spectrometry (HRMS) on several RDCs that degraded over the course of the targeted study to identify RDC TPs produced under different storage conditions. Finally, we conducted NTA of the standard mixture of 31 RDCs under five solvent conditions stored at room temperature. Through these approaches, we aim to determine optimal storage conditions for samples containing RDCs and to understand TP formation in stored samples, which in turn will increase the accuracy of future quantitative studies by reducing false positives. Moreover, this work highlights the role of environmental factors such as temperature and acidity and how they impact the formation of TPs under simplified conditions leading to a better understanding of RDC interactions.

2 Materials and methods

2.1 Chemicals

Standards for the RDCs were purchased from a variety of sources which can be found in Table S1. Optima grade water, formic acid, methanol and hydrochloric acid were all purchased from Fisher Scientific (Pittsburg, PA USA). Glutathione was purchased from TCI America (Portland, OR USA).

2.2 Solvent conditions for targeted degradation experiments

Degradation experiments were performed on mixtures of RDC standards under different solvent conditions. Five solvents (methanol, DI water, DI water acidified to pH = 2, methanol with 12.3 μg mL^{-1} glutathione, and DI water with 12.3 μg mL^{-1} glutathione) were prepared in duplicate in 10 mL volumetric flasks before being transferred into 20 mL amber vials with ambient atmosphere in the headspace. Each flask was spiked with 1.0 mL of a 2500 ng mL^{-1} native standard mixture and 0.2 mL of a 5000 ng mL^{-1} isotopically labeled internal standard mixture with a final concentration of 250 ng mL^{-1} and 100 ng mL^{-1}, respectively. The final concentration for the glutathione solution was 12.3 μg mL^{-1} matching previous publications.[34] Standard mixtures can be found in Table S2. The samples were stored in the dark at three temperatures: 22.2 °C (room temperature, RT), 4 °C (refrigerator, RF) and −20 °C (freezer,

FZ). The samples were only removed from these conditions to prepare aliquots for analysis.

2.3 Solvent conditions for individual standard degradation experiments

Degradation experiments were also performed on individual RDC standards under different solvent conditions to investigate transformation products. Five RDCs were chosen based on degradation in targeted experiments. 2-Mercaptibenzothiazole (MBT), hexamethoxymethylmelamine (HMMM), 4-nitroso-diphenylamine (4s DPA), 4-aminodiphenylamine (4-ADPA), 2,2,4-trimethyl-2,4-hydroquinoline (TMQ), and oligomeric-TMQ samples were prepared in triplicate in 10 mL volumetric flasks before being transferred into 20 mL amber vials. MBT and 4-ADPA samples were prepared in DI water, while HMMM, 4s DPA, TMQ and oligomeric-TMQ were prepared in DI water acidified to pH = 2. Each flask was spiked with 0.8 mL of a 25 000 ng mL^{-1} native standard and 0.2 mL of a 5000 ng mL^{-1} DPG-d10 standard with final concentrations of 2000 ng mL^{-1} and 100 ng mL^{-1}, respectively. The samples were stored at 22.2 °C in a dark space.

2.4 Targeted and non-targeted stability timepoints

The targeted analysis sampling points were Day 0, 1, 2, 8, 14, 21, 29, 43, and 71. The first three sampling points were clustered around the period expected for many of the PPD-related materials to transform.[18,31–33] Continued points were taken to examine the long-term stability of other rubber derived compounds. Non-target sampling points were Day 0, 2, 23, and 33, chosen based on results of the targeted study while the non-target sampling point for the standard mixture was on day 159 after all other analyses had been completed.

2.5 Instrumental analysis

2.5.1 Targeted analysis. The samples were analyzed using a high-performance liquid chromatograph (Agilent 1200 series) coupled to a triple quadrupole tandem mass spectrometer (Thermo Fisher Scientific TSQ Altis). Chromatography was performed using an Agilent InfinityLab Poroshell 120 EC-C18 column (2.1 × 50 mm, 2.7 μm) fitted with a C18 (2.1 mm, 2.7 μm) guard column. The column compartment was set to 45 °C with an injection volume of 1 μL. Mobile phases were water with 0.1% formic acid (A) and methanol with 0.1% formic acid (B) with a flow rate of 0.6 mL min^{-1}. Gradient and electrospray ionization details can be found in Table S3. The mass spectrometer was run in multi-reaction monitoring (MRM) mode with 42 precursors with a cycle time of 0.8 seconds. Precursor and product ion details can be found in Table S4.

2.5.2 Non-targeted analysis. The samples were analyzed using an ultra-high-performance liquid chromatograph (Thermo Fisher Scientific Vanquish Flex) coupled to a quadrupole-orbitrap mass spectrometer (Thermo Fisher Scientific Exploris 240 Orbitrap). Chromatography was performed using an Agilent Zorbax RRHD Eclipse Plus C18 column (2.1 × 100 mm, 1.8 μm) fitted with an C18 guard column (2.1 mm, 1.8 μm). The column compartment was set to 45 °C with an injection volume of 1 μL.

Mobile phases were water with 0.1% formic acid (A) and methanol with 0.1% formic acid (B) with a flow rate of 0.4 mL min^{-1}. Gradient and electrospray ionization details can be found in Table S5. Data acquisition used full scan mode and data dependent mode. Details for each mode can be found in Table S6. An exclusion list was created before each sequence by running a methanol solvent blank twice, averaging the spectrum, and adding any masses over 1×10^6 to the exclusion list.

2.6 Data processing

2.6.1 Targeted quantitation. Fragmentation collision energy was optimized for each standard *via* direct infusion to yield two high-intensity product ions for quantitation and qualification. Compounds were identified based on the retention time and MS/MS transitions. Quantitative analysis was performed using Skyline-daily (Version 25.1.1.206). A ten-point calibration curve (0.1, 0.5, 1.0, 5.0, 10, 25, 50, 100, 250, and 500 ng mL^{-1}) was prepared using a standard mixture to quantify across four orders of magnitude. The peak area of the quantitative product ion was ratioed with their corresponding isotopically labeled internal standard and plotted against the analyte concentration. Calibration points were excluded if the accuracy of the calculated value was outside 15% of the theoretical value. Limits of detection (LODs) were calculated by using eqn (1). Limits of quantification (LOQs) were calculated by using eqn (2). Whenever a negative limit of detection was calculated, the lowest viable calibration point was chosen as the LOD, with the LOQ three times that value.

$$\text{LOD} = \text{blank} + 3 \times \text{standard deviation} \quad (1)$$

$$\text{LOQ} = \text{LOD} \times 3 \quad (2)$$

To account for concentrations under the LOD/LOQ when calculating percent difference, the LOD was divided by two with the resulting value[36] used in place of the original value. Percent difference was calculated by using eqn (3) using the day 0 normalized concentration data (ng mL^{-1}) and the Day 71 normalized concentration data (ng mL^{-1}).

$$\text{Percent difference} = |((\text{Day 71} - \text{Day 0})/\text{Day 0}) \times 100| \quad (3)$$

2.6.2 Non-targeted analysis. Compound Discoverer (Version 3.3.3.200) was used to process the raw data files. Only features with a peak area ratio 5 times that of the blank and exhibiting MS2 spectra were considered for identification. Prioritization was given to features that were intense across multiple samples. Features not identified with Compound Discover were investigated with *in silico* tools *via* SIRIUS CSI:-Finger ID[37–39] (Version 6.3.0) and MetFrag[40] (Version 2.6.8) for further structural elucidation.

2.6.3 Inter-/intra-day precision. Precision was determined by running samples at two concentration levels, 5 ng mL^{-1} and 100 ng mL^{-1}, on the same day ($n = 5$) and over several days ($n = 3$). The results are expressed in relative standard deviation (% RSD) and can be found in Table S7.

3 Results and discussion

3.1 Targeted stability study

3.1.1 Isotopically labeled internal standard pairings. We first evaluated the validity of internal standard pairings, because most RDCs are still "emerging" contaminants and do not have isotope labeled standards, and we had to rely on a small subset of isotope labeled standards. The outliers (Fig. 1a) stem from the behavior of the isotopically labeled standard chosen to normalize the peak areas of the native standards. Initial pairings of isotopic labeled standards were based on physiochemical properties and structural similarities. These pairings were not always successful. Instability in the isotopically labeled standards led to two types of problems when paired with native standards. TMQ paired with TMQ-d4 displays the first type of issue, with TMQ-d4 increasing sharply under one condition where TMQ did not. This led to an artificial decrease in normalized peak area for TMQ which was mitigated by switching to an isotopically labeled standard that was more stable. MBT paired with MBT-d4 displays the second issue where both standards decreased over the course of the experiment. This masked the degradation of MBT when looking at the normalized peak area and was only caught when checking over the raw peak areas. All standards were eventually paired to either 6PPD-Q-d5 or DPG-d10 as the two matched the raw peak area trends of the RDCs well. Care must be taken when choosing isotopic labeling pairings, as the above examples show that the "ideal" pairings can alter data depending on the design of the study. All compounds matched to 6PPD-Q-d5 saw a sharp increase in raw peak area on day 71. While the raw peak area of 6PPD-Q-d5 increased as well, the −20 °C in the water sample increased at a reduced slope and the 22.2 °C in acidified water saw no increase at all. This caused the normalized peak area of DPPD, 4-phenylazodiphenylamine, and *N*-phenyl-1-naphthylamine to increase artificially which affected their calculated concentrations. 6PPD-Q day 0 data were <LOD and an outlier when compared to the other 6PPD-Q data points. All analyses using 6PPD-Q utilize day 1 data.

3.1.2 Optimal storage conditions and compound class trends. We observed the lowest percent change for all compounds in methanol stored at −20 °C in the dark, with a median 3.5% difference (SD = 4.2%) over the 71 day period (Fig. 1a). Temperature had less of an effect on stability than we initially expected, with most stability being dictated by solvent conditions rather than the temperature of storage. However, several compounds (TMQ, MBT, and IPPD) demonstrate a trend under certain conditions where higher temperatures lead to a larger percent difference (Fig. 1b).

The most stable compound classes were benzothiazoles and diphenyl guanidine (Fig. 1b). These compounds are typically added into rubber as accelerants for the vulcanization process. Benzothiazoles had a median 5.8% difference (SD = 2.9%) under all conditions, while diphenyl guanidine had a median 4.6% difference (SD = 3.4%) under all conditions. This stability, alongside leaching behavior and abundance in rubber particles, may play a role in their environmental prevalence as many
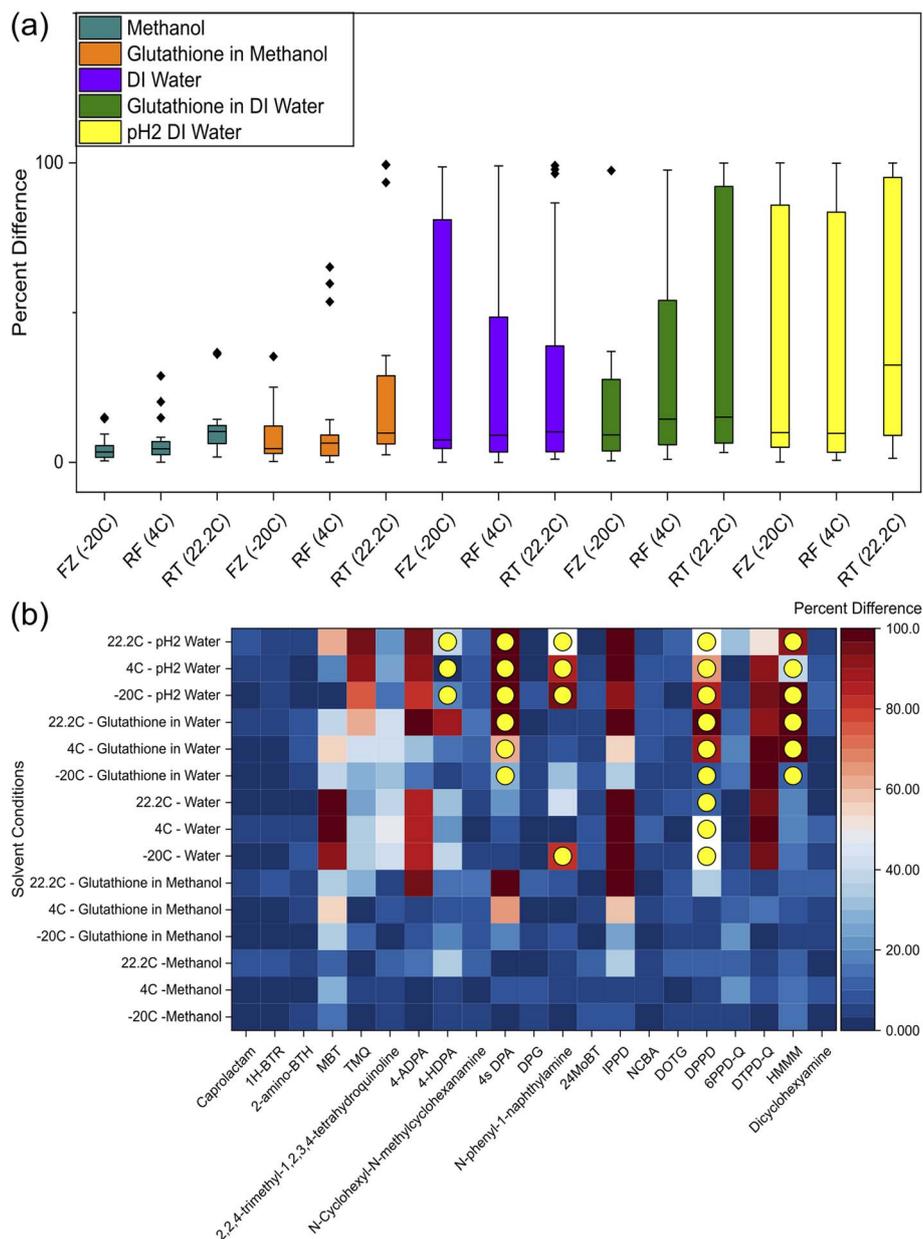
Fig. 1 Day 0 and Day 71 percent difference for all quantitative compounds ($n = 21$) grouped based on the experimental condition (a) and Day 0 and Day 71 percent difference for all quantitative compounds ($n = 21$) under each experimental condition (b). Compounds that immediately degraded under the initial conditions sometimes showed low percent differences. To account for this, any compound that fell below 45% of the expected 250 ng mL^{-1} value was flagged. These compounds and conditions can be found in Table S8 and are marked with yellow circles in Fig. 1b.

studies have identified these compound classes in their samples.[41–44]

Antioxidants and their derivatives were most active for transformation, with every antioxidant showing drastic differences under at least one solvent condition. The most common condition for transformation to occur was pH = 2, indicating the incompatibility of acidified media for storage. Two TPs of antioxidants, DTPD-Q and 4-HDPA, transformed under similar conditions. 6PPD-Q was the exception, remaining stable under all conditions. Trends amongst PPDs are explored further below.

3.1.3 Compound trends. 6PPD and DTPD used a semi-quantified method (peak areas normalized to an isotopically labeled internal standard) due to accuracy issues with the calibration curve. Calibration points failing to meet the 15% accuracy criterion resulted in calibration curves with fewer than five acceptable points, precluding quantitative analysis. For these compounds, normalized peak areas were reported instead of absolute concentrations and as such were not included with the rest of the quantitative data. Trend data can be seen in Fig. S1 and S2. Solvent conditions affect DTPD and DPPD stability, with methanol conditions remaining inactive
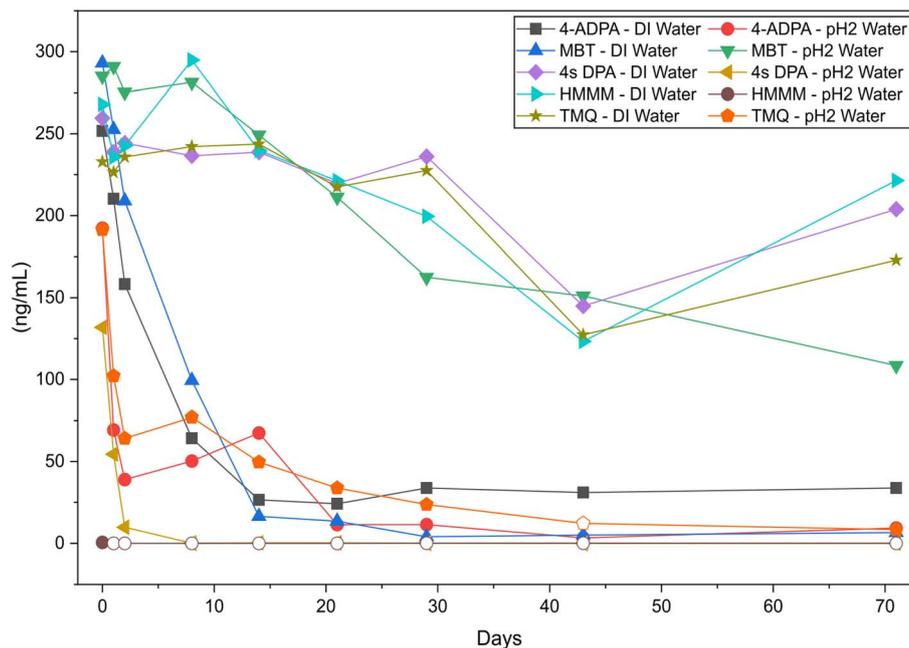
Fig. 2 Five rubber derived compounds (4s DPA, 4-ADPA, MBT, TMQ, and HMMM) that showed a drastic decrease over a 71 day period under two conditions (DI water and DI water adjusted to pH = 2). Any point that was <LOQ was plotted with no color fill.

compared to water conditions, which showed transformation. Both solvent and temperature conditions affect 6PPD stability. DI water and pH = 2 conditions led to transformation regardless of temperature (median 99% difference; SD = 0.13%). The stability in solvents with the addition of glutathione, regardless of solvent, was dictated by temperature with 22.2 °C solvent conditions experiencing more transformation (median 99% difference; SD = 0.033%) in contrast to −20 °C (median 68% difference; SD = 12%). Methanol solvent conditions were likewise affected by temperature with 22.2 °C conditions experiencing a 72% difference while −20 °C conditions only experienced a 2.6% difference. IPPD showed a similar transformation profile to 6PPD. The differences between 6PPD/IPPD and DTPD/DPPD may be due to slight structural differences with DTPD/DPPD having an additional benzene ring, while 6PPD/IPPD has branching alkyl chains. Notably, the stability of PPDs did not improve when using modified matrices (addition of glutathione at 12.3 μg mL^{-1}, acidification). It is possible that glutathione can protect individual RDC standards and this protection is being masked by other interactions within the RDC mixtures. It is also possible that glutathione did protect the PPDs from ozonation and they transformed *via* another pathway, but this was not examined within our study. Recent publications have seen more success with protecting PPDs with the antioxidant shield method.[45] The 12.3 μg mL^{-1} of glutathione used in this study is not sufficient for protection in RDC mixtures and concentrations below 12.3 μg mL^{-1} will likely see similar results.

Exceptions are found for most active and inactive groups. While most benzothiazoles were found to be inactive for transformation, MBT was found to be active under DI water conditions (median 98% difference; SD = 3.3%). The reactivity

of MBT compared to the other MBTs may be due to the strong nucleophilic nature of the additional sulfur attached to the benzothiazole backbone. The other BTH compounds were TPs or impurities of other vulcanizing agents, NCBA and 2-amino-BTH from CBS and 24MoBT from OBS.[46] This transformation led to less reactive products (we hypothesize either based on steric bulk or lessened nucleophilicity) which no longer react under the conditions we tested. Several of these compounds are commonly found in tire leachate[17,47–49] and have been considered markers for tire contamination.[46,50]

One group of antioxidants remained inactive for transformation during the experiment. Dicyclohexylamine and *n*-cyclohexyl-*n*-methylcyclohexanamine remained inactive (median 7.3% difference; SD = 4.4%) under all conditions. We postulate that the lack of the amine group in the para position (compared to compounds like 4-ADPA) lessens the reactivity of the compounds.

In addition to antioxidant TMQ, its analog 2,2,4-trimethyl-1,2,3,4-tetrahydroquinoline was included to investigate the role that small structural differences may play in transformation. The two compounds exhibit different stabilities in the matrices. While TMQ transforms under low pH conditions, 2,2,4-trimethyl-1,2,3,4-tetrahydroquinoline does not. The only structural difference between the two is a double bond between the three and four positions on TMQ. This bond is the site of transformation for several TPs, discussed further in Section 3.2.1. Structures of both compounds and their trends over the experiment can be found in Fig. S3.

3.1.4 Selected compounds for transformation study. In addition to PPDs and their transformation products, five rubber derived compounds, 4-ADPA, MBT, 4s DPA, HMMM, and TMQ, were also shown to degrade over time (Fig. 2).
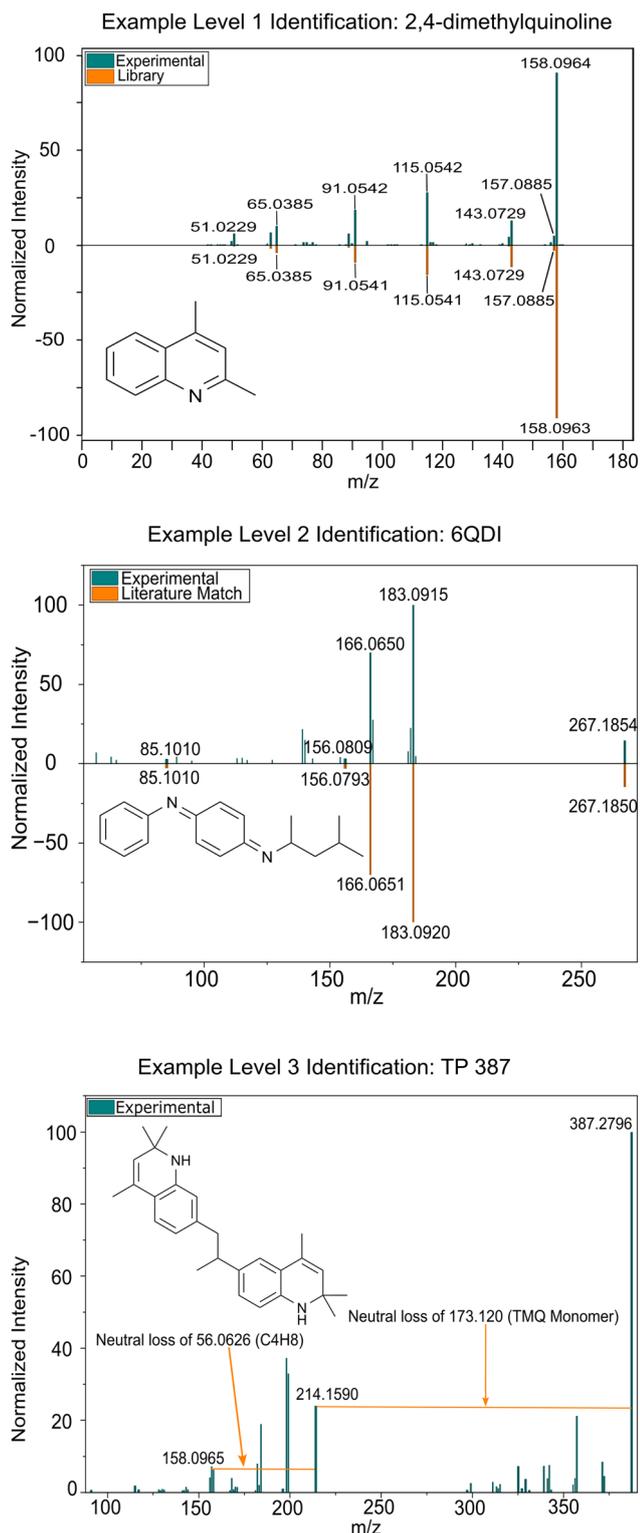
Fig. 3 Examples of TPs across three confidence levels seen across the two data sets. 2,4-Dimethylquinoline was shared between both data sets while 6QDI and TP 287 were exclusive to the mixed standard set and the single standard set respectively.

These compounds are structurally diverse, except for 4-ADPA and 4s DPA which only differ in a single functional group. Despite this, the conditions under which these compounds transform still differ. The roles that these RDCs play in tire production all vary as well. Their uses include vulcanization accelerators (MBT), curative agents with activated silica (HMMM), and antioxidants (4s DPA, 4-ADPA, and TMQ).[5,51] RDCs can be present as both parent compounds and TPs of other RDCs; for example, while 4-ADPA and 4s DPA are additives used during manufacturing, they are also TPs of 6PPD. The lack of structural similarity and industrial role between these five compounds indicate that there is no clear trend specific to structural configurations or use in tire manufacturing for this degradation. The exact mechanisms behind the degradation of these RDCs were not fully confirmed within this study. Later NTA experiments (Section 3.2) revealed that demethylation occurred in both HMMM and TMQ, while hydrolysis occurred in 4-ADPA, 4sDPA, and MBT. 4-ADPA was only examined under neutral conditions so the degradation pathway under acidic conditions remains unexplored. Given the structural similarity to 4sDPA it is plausible that hydrolysis was the cause behind the degradation.

3.2 Non-targeted identification of TPs from single standards

3.2.1 Feature prioritization for TPs. Non-target analysis was performed on solutions of individual standard compounds stored in water and pH = 2 water at 22.2 °C over 33 days to investigate TP formation. Features exhibiting MS2 spectra with peak area ratios of the sample to solvent blank greater than or equal to 5 were considered for further analysis. Feature prioritization was done for each standard per day by sorting by the peak area and adding the top six features into a list to focus on the most abundant transformation products.

Initial prioritization yielded 65 total features across all six standards, with this number decreasing to 36 after in-source fragments were identified and removed. Of the 36 features of interest, 21 were determined to be TPs, and 15 were determined to be fast forming TPs or impurities. These classifications were determined *via* the change in peak area over the course of the experiment. Impurities showed no change in peak areas, fast forming TPs/impurities decreased from the day 0 peak area, and TPs increased over the entire experiment or decreased after an initial increase. Compound annotations were assigned based on the Schimanski schema[52] (Fig. 3) and can be found in Table S11.

3.2.2 4-ADPA. While 4-ADPA transforms under both DI water and pH = 2 water conditions, DI water was chosen because of its relevance to environmental conditions. Out of the six TPs for 4-ADPA, we confirmed only 4-hydroxydiphenylamine (4-HDPA) with level one confidence (Fig. 4 and S6). Other transformation products such as TP 396 and TP 363 share a common fragment, m/z 167.072, with 4-ADPA. Their larger molecular size suggests formation *via* aggregation, though the exact mechanism was not explored further. Other TPs lack fragmentation similarities with 4-ADPA and we believe them to have more unique structural transformations.

3.2.3 4s DPA. Under acidic conditions, 4s DPA transforms quickly with most changes in peak area occurring over the first two days (Fig. 2). The resulting products are 4-aminophenol and
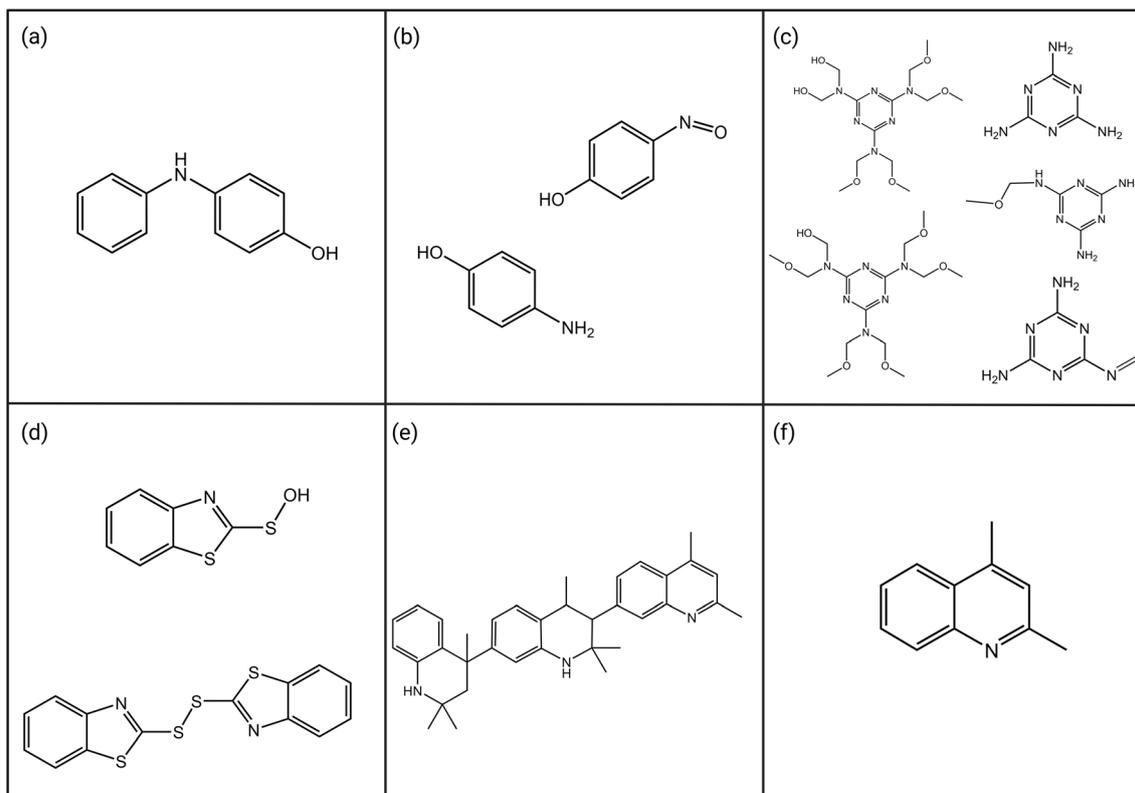
Fig. 4 High confidence transformation products for (a) 4-ADPA, (b) 4s DPA, (c) HMMM, (d) MBT, (e) oligomeric-TMQ, and (f) TMQ.

4-nitrophenol (Fig. 4), produced *via* acid hydrolysis (addition of hydroxyl groups on the benzene ring). We also identified numerous impurities/fast forming TPs within the solution (on Day 0), including 4-ADPA (level 2b) and a likely positional isomer at a later retention time (level 3). Both TPs decrease over the initial few days until they are no longer detectable at the day 23 sampling point. We also identified a second positional isomer pair, TP 183a and TP 183b. Their fragmentation patterns are identical (Fig. S4), and share similarities to 4-ADPA in the higher *m/z* region of the MS2 spectra (*m/z* fragments 167.0728 and 139.0542) leading to compound elucidation to focus on the diphenylamine backbone.

3.2.4 MBT. While the quantitative portion of the study indicated that MBT decreases under aqueous conditions, we saw minimal loss over the course of the transformation study. We identified two TPs, TP183d and 2,2-dithiobis(benzothiazole) (MBTS) (Fig. 4). However, the formation of these TPs does not explain the large losses seen during the quantitative study. We hypothesize that the loss of MBT in the targeted portion of the study to be due to inter-compound interactions within the mixture of 31 compounds rather than transformations caused by the matrix. This highlights that cross-reactivity in mixtures of compounds may contribute to TP formation not seen in solutions of individual standards, and therefore has important implications for the transformations of real-world samples. TP183d is formed *via* a hydrolysis mechanism (addition of a hydroxyl group on the thiol group) and increased in peak area over the first three sampling points before decreasing in peak

area on the day 33 sampling point, suggesting a potential secondary transformation process. 2,2-Dithiobis(benzothiazole) is formed *via* oxidation, consistent with other studies,[53–55] over the first two sampling points before decreasing in peak area over the second two sampling points. Five other compounds that coeluted with MBT were identified with level 5 confidence.

3.2.5 HMMM. The molecular structure of HMMM contains a melamine core modified with methoxymethyl groups attached to each amine. Transformation for HMMM begins with each methoxymethyl group demethylated.[56] The resulting TPs are smaller in mass and elute earlier, suggesting greater polarity. As described above, the demethylation of a methoxymethyl group results in TP 377 and TP 363 which were only found on the day 0 sampling point. No new TPs were seen on day 2. TPs found on day 23 and day 33 were eluting earlier and were closer to the melamine core in structure. TP 183c remained near constant across both points. Rather than the TP being stable, the likely cause of the constant peak area is that the rate of degradation from larger TPs matches the rate at which TP 183 is transforming into smaller species. The final TPs seen in the study included *N*-(methoxymethyl)-1,3,5-triazine-2,4,6-triamine (MonoMMM), methylene melamine, and melamine (Fig. 4).

3.2.6 Monomer-TMQ. TMQ transformed over the course of the study to 2,4-dimethylquinole (2,4-DMQ, level 1 ID) *via* demethylation at the 2-positions on TMQ and was the major TP of TMQ monomer. This is to the best of our knowledge, the first piece of evidence revealing 2,4-DMQ as a TP of TMQ (Fig. 4). We identified two other TPs, TP 359 and TP 361. TP 359's poor MS2
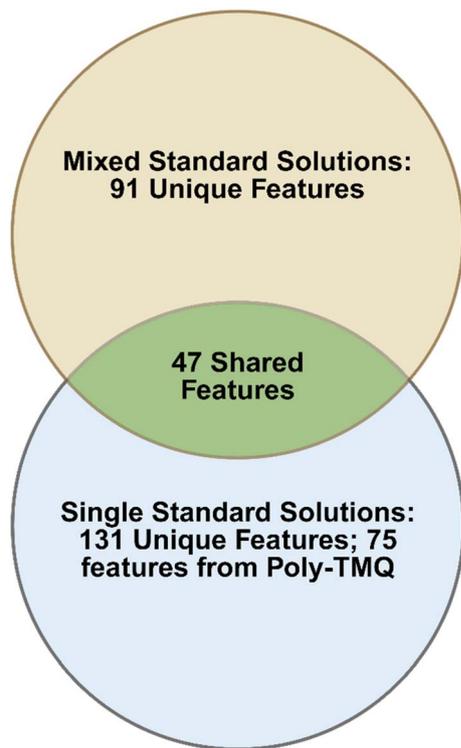
Fig. 5 Venn diagram of the single standard data set compared to the mixed standards data set. Once features only found in the oligomeric-TMQ standard were removed, single standard solutions only had 56 unique features compared to 91 unique features from mixed standards.

spectrum hindered structural identification, but the larger molecular mass indicates that it is likely an aggregation product similar to TP 361. TP 361 is a possible aggregate which was identified as a hydrolyzed TMQ-dimer, though the position of this functional group remains ambiguous.

3.2.7 Oligomeric-TMQ. We identified 4 different oligomers alongside the TMQ monomer in an oligomeric-TMQ standard of unknown chain length. We expected that the degradation of the oligomeric-TMQ would lead to an increase in monomer TMQ. However, the peak area for monomer TMQ decreased over the course of the study, suggesting that oligomeric-TMQ produced different TPs. Moreover, the oligomers do not seem to break down. Two TPs, TP 331 and TP 507, are two oligomers whose end terminal monomer TMQs were converted to 2,4-DMQ (Fig. 4).

3.3 Non-targeted study of the standard mixture

3.3.1 Prioritization of features. Non-target analysis was performed on solutions containing 31 compounds stored under five conditions (methanol, water, water adjusted to pH = 2, methanol with glutathione addition, and water with glutathione addition) at 22.2 °C over 159 days to investigate transformation product formation. Features exhibiting MS2 spectra with peak area ratios of the sample to solvent blank greater than or equal to 5 were considered for further analysis. Initially, we found a total of 253 features across the 5 solvent types. Removing in-

source fragments, adducts, and glutathione related features reduced the number of features to 138.

3.3.2 NTA feature comparison and storage artifacts. We overlayed the potential TP features in the mixture experiment and single standard experiments (Fig. 6) to identify shared features. 47 features were found in both data sets including melamine, methoxymethylmelamine, 4-aminophenol, 2,4-DMQ, TP183d, and 2,2-dithiobis(benzothiazole). Of these shared features, 28 were confirmed TPs, 18 were fast forming TPs/impurities, and 2 were impurities (Table S9). The majority stemmed from parent compounds TMQ (13 features) and 4-ADPA (14 features). The shared TPs are likely due to common transformations such as hydroxylation and may be seen in environmental samples. However, the complexity of environmental matrices may preclude the formation of such TPs.

Each data set contains unique features with the mixed standards containing 91 unique features, and the single standards containing 131 unique features (Fig. 5). Since the 91 mixture-exclusive features are likely reaction products from different rubber additives, they remain poorly characterized but may have environmental significance. After further examining the 131 single standard features, we found that 75 of them stem from oligomeric-TMQ. It is likely that some of these features are isomers, or in-source fragments, but due to poor chromatic resolution and complexity of the oligomeric standard, further investigation was not carried out. With over a third of all features stemming from only five compounds, many environmentally prevalent TPs may stem from only a handful of RDCs. Features from both datasets were compared with a third dataset generated by McMinn *et al.*[57] to check for environmental occurrence. 20% of the single standard features (8 of 40) were seen in the environmental samples, exclusively stemming from MBT and oligomeric-TMQ. Only 6.4% of the mixed standard features (9 of 141) were seen in the environmental samples, with the majority being artifacts of storage.

3.3.3 Feature trends and identifications. Trends related to molecular weight (MW) and retention time (RT) were examined as many features could not be assigned structures. Comparing the standards (median RT of 6.37 and median MW of 211) with the features (median RT of 7.19 and median MW of 296) shows a trend of increasing molecular weight and retention time. While this may involve smaller additions such as the addition of oxygen or a methyl group, we see some cases where parent compounds are aggregating together with minimal structural changes. This can occur between a single compound or between two or more compounds with the most frequently seen being MBT and 4-ADPA. This is no surprise given the instability exhibited by these compounds in previous experiments. Feature 351 and feature 516 are two examples of aggregation between two compounds unique to the mixed standards. Both have a 4-HDPA backbone to which one (feature 351) or two (feature 516) MBTs attach to. For both features, the most intense fragment peaks are those corresponding to the neural loss of MBT (Fig. 6). Features 381b and 545 are examples of aggregation between the same compound (4-ADPA). 318b consists of a 4-ADPA dimer with the addition of an oxygen, while 545 is a 4-ADPA trimer. For both features, the most intense fragment peaks are those
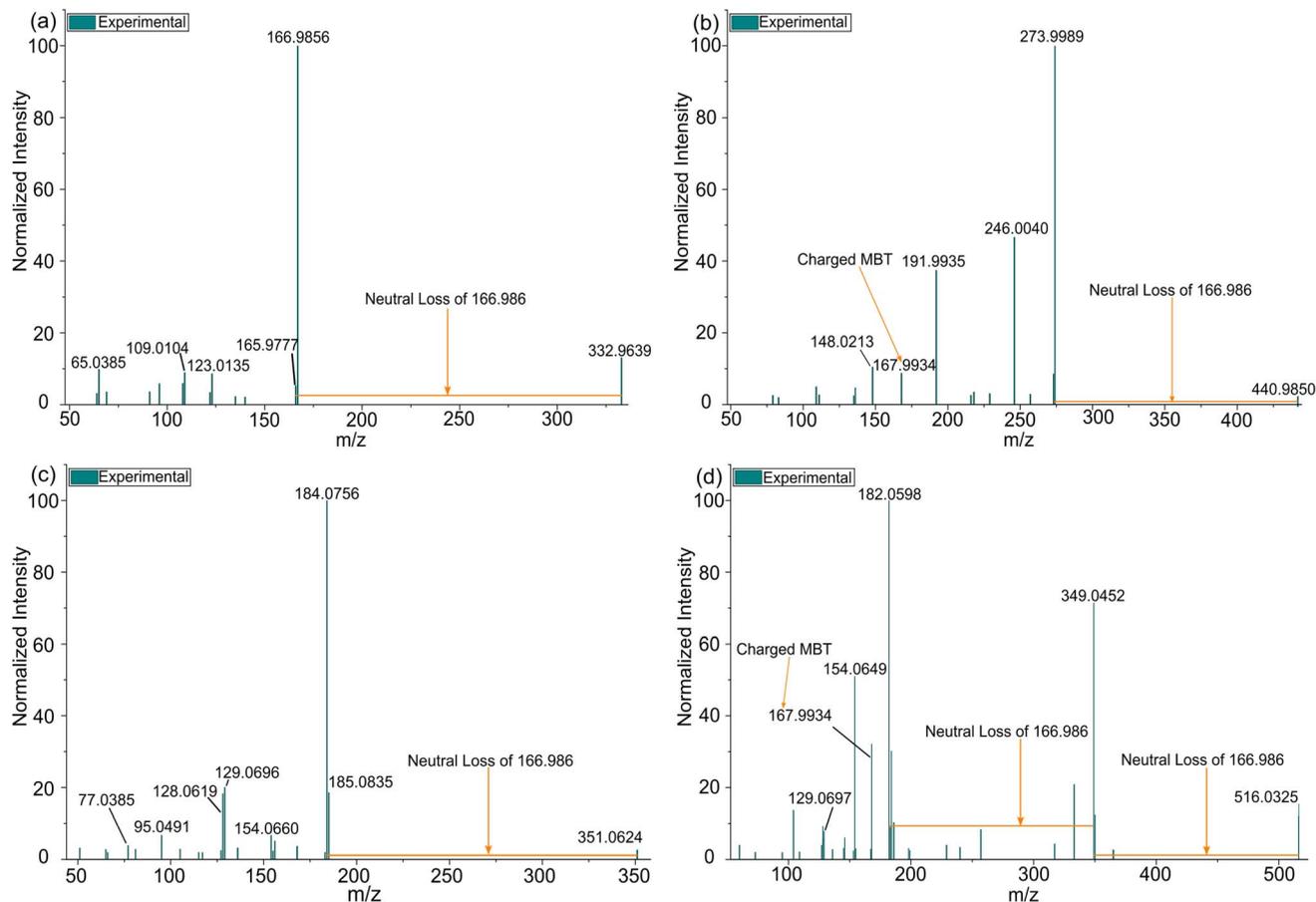
Fig. 6 Mass spectra of four MBT related TPs, (a) 2,2-dithiobis(benzothiazole), (b) feature 440, (c) feature 351, and (d) feature 516. The neutral losses/charged ions of MBT are displayed in orange in the figure.

corresponding to the neural loss of benzene rings and phenyl-amine radicals in line with losses seen from 4-ADPA (Fig. S5). Moreover, both solvents (water and methanol) with glutathione addition contained feature 361 and feature 490, bicyclic amines that linked with fragments of glutathione. Future work utilizing antioxidants as stabilizing agents should be wary of trans-formations between said antioxidants and the target chemicals. Additional insights were that water conditions led to the addi-tion of carboxylic acid and ketone functional groups, while acidified water conditions led to modifications to the benzo-thiazole compound class.

No MBT related TPs were identified under water conditions only, despite interest stemming from a lack of transformation found in Section 3.2.4 of this paper. MassQL[58] was used to identify compounds that contained MBT indicators (neutral loss of 166.986 or a product ion with an m/z 167.993). After false positives were removed, 12 features were identified with two shown in Fig. 6. They were found mainly under methanol and water conditions simultaneously, or alone under pH = 2 conditions. It is possible that the TPs were filtered out and thus were not seen during feature elucidation.

After structural annotations were complete, 1 level 1 compound, 10 level 2a features, 26 level 3 features, 61 level 4 features, and 41 level 5 features were identified. Level 1

identifications are confirmed by using the standard reference, with 2,4-DMQ being the sole identification. Level 2a is confirmed by a spectral library match or *via* matching literature. Examples of these identifications are 6QDI, methoxymethylmelamine, and 4-(4-methylanilino)phenol. Level 3 identifications are supported by *in silico* fragmentation and manual structure elucidation. See Table S10 for all features and their annotations.

4 Limitations, conclusions, and future work

Due to resource limitations, samples were run in experimental duplicates, preventing more rigorous statistical analysis. Inclusion of acetonitrile as a solvent condition would have provided insight into the differences in stability for RDCs in protic *vs.* aprotic solvents. This may be important for future work as the two most common solvents used for 6PPD analysis are methanol and acetonitrile.

Another limitation within this study was the ambient atmosphere in the headspace above each sample. With each aliquot taken the atmosphere in the headspace was renewed, increasing the oxygen availability in our experiment. These conditions likely played a role in the degradation of the various antioxidants and in the formation of transformation products

such as 2,2-dithiobis(benzothiazole). If samples are stored under anoxic conditions (inert gas or no headspace) we would expect a reduction in the formation of transformation products which rely on oxidation. Some RDCs could also exhibit a decreased rate of degradation, but other degradation pathways could mask this occurrence.

Our multi-month study of RDCs under 5 matrix conditions at three different temperatures revealed that samples stored in methanol at temperatures $\leq -20\ ^\circ$C are most stable over long periods of time. Acidification results in rapid transformation of numerous RDCs, and thus should be avoided if possible. Addition of glutathione failed to prevent degradation of PPDs and resulted in TPs between RDCs and glutathione fragments. Quantification of certain rubber derived compounds such as PPDs will be difficult unless they are reconstituted in an organic solvent or ran immediately after sampling.

Between the two non-targeted datasets, 42 features were identified at level 3 confidence or higher. 2,4-DMQ was identified as a TP of TMQ with level one confidence. Transformations unique to each standard mix were seen, with 91 features exclusive to mixed standards while 56 were exclusive to single standards excluding oligomeric-TMQ. Features unique to the mixed standards likely stem from reactions between RDCs. While this work was completed under simplified conditions, these understudied TPs may have environmental relevance.

Author contributions

Phillip Berger: conceptualization, formal analysis, methodology, investigation, validation, visualization, writing – original draft, writing – review & editing. Katherine Poisson: methodology, writing – review & editing. Jamie Adams: visualization, writing – review & editing. Zhenyu Tian: conceptualization, supervision, writing – original draft, writing – review & editing.

Conflicts of interest

There are no conflicts to declare.

Data availability

The data supporting this article have been included as part of the supplementary information (SI). Supplementary information: stability trend data for select rubber-derived compounds under various storage conditions, fragmentation evidence supporting the structural assignment of key transformation products, and annotated mass spectra documenting compound identifications at confidence levels 1 through 3. SI tables provide analytical method details including instrument parameters, chromatographic gradients, and electrospray settings for both targeted and non-targeted acquisition, along with standard preparation information. Additional tables report method performance metrics, compound identification confidence levels for detected features, and quantitative and semi-quantitative data for targeted and non-targeted compounds across storage conditions. See DOI: https://doi.org/10.1039/d5em01025j.

References

1 World Motor Vehicle - Sales - 2024; International Organization of Motor Vehicle Manufacturers (OICA), https://oica.net/sales-statistics/, accessed September 2025.

2 W. W. Barbin and M. B. Rodgers, 9 - The Science of Rubber Compounding, in *Science and Technology of Rubber*, ed. J. E. Mark, B. Erman and F. R. Eirich, Academic Press, San Diego, 2nd edn, 1994, pp 419–469, DOI: 10.1016/B978-0-08-051667-7.50014-7.

3 A. Wik and G. Dave, Occurrence and Effects of Tire Wear Particles in the Environment – A Critical Review and an Initial Risk Assessment, *Environ. Pollut.*, 2009, **157**(1), 1–11, DOI: 10.1016/j.envpol.2008.09.028.

4 S. Wagner, T. Hüffer, P. Klöckner, M. Wehrhahn, T. Hofmann and T. Reemtsma, Tire Wear Particles in the Aquatic Environment - A Review on Generation, Analysis, Occurrence, Fate and Effects, *Water Res.*, 2018, **139**, 83–100, DOI: 10.1016/j.watres.2018.03.051.

5 M. Sheridan, *The Vanderbilt Rubber Handbook*, 14th ed.

6 M. L. Kreider, J. M. Panko, B. L. McAtee, L. I. Sweet and B. L. Finley, Physical and Chemical Characterization of Tire-Related Particles: Comparison of Particles Generated Using Different Methodologies, *Sci. Total Environ.*, 2010, **408**(3), 652–659, DOI: 10.1016/j.scitotenv.2009.10.016.

7 A. Dahl, A. Gharibi, E. Swietlicki, A. Gudmundsson, M. Bohgard, A. Ljungman, G. Blomqvist and M. Gustafsson, Traffic-Generated Emissions of Ultrafine Particles from Pavement–Tire Interface, *Atmos. Environ.*, 2006, **40**(7), 1314–1323, DOI: 10.1016/j.atmosenv.2005.10.029.

8 G. Cao, W. Wang, J. Zhang, P. Wu, X. Zhao, Z. Yang, D. Hu and Z. Cai, New Evidence of Rubber-Derived Quinones in Water, Air, and Soil, *Environ. Sci. Technol.*, 2022, **56**(7), 4142–4150, DOI: 10.1021/acs.est.1c07376.

9 M. Polukarova, E. L. Gaggini, E. Rødland, E. Sokolova, M. Bondelind, M. Gustafsson, A.-M. Strömvall and Y. Andersson-Sköld, Tyre Wear Particles and Metals in Highway Roadside Ditches: Occurrence and Potential Transport Pathways, *Environ. Pollut.*, 2025, **372**, 125971, DOI: 10.1016/j.envpol.2025.125971.

10 T. R. Barber, F. Ribeiro, S. Claes, Y. Kawamura, J. Yeung, H. A. Byrne, S. Weyrauch, T. Reemtsma and K. M. Unice, The Identification and Quantification of Tire and Road Wear Particles in Osaka Bay, Japan, by Two Analytical Methods, *Mar. Pollut. Bull.*, 2025, **211**, 117363, DOI: 10.1016/j.marpolbul.2024.117363.

11 A. D. Gray, H. Wertz, R. R. Leads and J. E. Weinstein, Microplastic in Two South Carolina Estuaries: Occurrence, Distribution, and Composition, *Mar. Pollut. Bull.*, 2018, **128**, 223–233, DOI: 10.1016/j.marpolbul.2018.01.030.

12 P. Klöckner, B. Seiwert, S. Wagner and T. Reemtsma, Organic Markers of Tire and Road Wear Particles in Sediments and Soils: Transformation Products of Major Antiozonants as Promising Candidates, *Environ. Sci. Technol.*, 2021, **55**(17), 11723–11732, DOI: 10.1021/acs.est.1c02723.

13 M. Kovochich, S. C. Oh, J. P. Lee, J. A. Parker, T. Barber and K. Unice, Characterization of Tire and Road Wear Particles in Urban River Samples, *Environ. Adv.*, 2023, **12**, 100385, DOI: 10.1016/j.envadv.2023.100385.

14 N. Evangeliou, H. Grythe, Z. Klimont, C. Heyes, S. Eckhardt, S. Lopez-Aparicio and A. Stohl, Atmospheric Transport Is a Major Pathway of Microplastics to Remote Regions, *Nat. Commun.*, 2020, **11**(1), 3381, DOI: 10.1038/s41467-020-17201-9.

15 L. A. Rasmussen, F. Liu, N. D. R. Klemmensen, J. Lykkemark and J. Vollertsen, Retention of Microplastics and Tyre Wear Particles in Stormwater Ponds, *Water Res.*, 2024, **248**, 120835, DOI: 10.1016/j.watres.2023.120835.

16 C. Rauert, N. Charlton, E. D. Okoffo, R. S. Stanton, A. R. Agua, M. C. Pirrung and K. V. Thomas, Concentrations of Tire Additive Chemicals and Tire Road Wear Particles in an Australian Urban Tributary, *Environ. Sci. Technol.*, 2022, **56**(4), 2421–2431, DOI: 10.1021/acs.est.1c07451.

17 K. Müller, D. Hübner, S. Huppertsberg, T. P. Knepper and D. Zahn, Probing the Chemical Complexity of Tires: Identification of Potential Tire-Borne Water Contaminants with High-Resolution Mass Spectrometry, *Sci. Total Environ.*, 2022, **802**, 149799, DOI: 10.1016/j.scitotenv.2021.149799.

18 Z. Tian, H. Zhao, K. T. Peter, M. Gonzalez, J. Wetzel, C. Wu, X. Hu, J. Prat, E. Mudrock, R. Hettinger, A. E. Cortina, R. G. Biswas, F. V. C. Kock, R. Soong, A. Jenne, B. Du, F. Hou, H. He, R. Lundeen, A. Gilbreath, R. Sutton, N. L. Scholz, J. W. Davis, M. C. Dodd, A. Simpson, J. K. McIntyre and E. P. Kolodziej, A Ubiquitous Tire Rubber–Derived Chemical Induces Acute Mortality in Coho Salmon, *Science*, 2021, **371**(6525), 185–189, DOI: 10.1126/science.abd6951.

19 E. Stephensen, M. Adolfsson-Erici, M. Hulander, J. Parkkonen and L. Förlin, Rubber Additives Induce Oxidative Stress in Rainbow Trout, *Aquat. Toxicol.*, 2005, **75**(2), 136–143, DOI: 10.1016/j.aquatox.2005.07.008.

20 P. J. Ankley, F. C. da Silva Junior, B. Hunnie, C. Roberts, A. N. M. Eriksson, E. Kohlman, J. Corker, J. Westcott, B. Germain, M. J. Martin, J. Dubiel, K. Anderson-Bain, R. M. Urrutia, N. Hogan, J. P. Giesy, S. Wiseman, E. Krol, M. Hecker and M. Brinkmann, The Xenometabolome of Early-Life Stage Salmonids Exposed to 6PPD-Quinone, *Environ. Sci. Technol.*, 2025, **59**(28), 14214–14225, DOI: 10.1021/acs.est.5c01442.

21 J. K. McIntyre, J. Prat, J. Cameron, J. Wetzel, E. Mudrock, K. T. Peter, Z. Tian, C. Mackenzie, J. Lundin, J. D. Stark, K. King, J. W. Davis, E. P. Kolodziej and N. L. Scholz, Treading Water: Tire Wear Particle Leachate Recreates an Urban Runoff Mortality Syndrome in Coho but Not Chum Salmon, *Environ. Sci. Technol.*, 2021, **55**(17), 11767–11774, DOI: 10.1021/acs.est.1c03569.

22 L. Tang, X. Li, S.-Y. Zhu, Y.-K. Wan, S.-K. Zhang, J.-Z. Ma, Y. Yang, A.-W. Chen, L. Luo and L.-Y. Cao, 6PPD and 6PPD Quinone Induce Endometrial Cell Dysfunction via Activating ERα and GPER at Human-Relevant Levels, *Environ. Sci. Technol.*, 2025, **59**(20), 9918–9929, DOI: 10.1021/acs.est.4c13961.

23 F. R. Harris, M. D. Jankowski, D. L. Villeneuve and J. A. Harrill, Phenotypic Profiling of 6PPD, 6PPD-Quinone, and Structurally Diverse Antiozonants in RTgill-W1 Cells Using the Cell Painting Assay, *Environ. Sci. Technol. Lett.*, 2025, **12**(6), 695–701, DOI: 10.1021/acs.estlett.5c00327.

24 B. Li, C. Xu, D. Zhang, S. Wang, J. Xu, B. Xiao, Y. Feng, H. Fu, X. Chen and Z. Zhang, Combined Analysis of Network Toxicology and Multiomics Revealed the Potential Mechanism of 6PPDQ-Induced Hepatotoxicity in Mice, *Environ. Sci. Technol.*, 2025, **59**(21), 10204–10214, DOI: 10.1021/acs.est.5c03906.

25 J. Le Du-Carrée, C. K. Palacios, A. Rotander, M. Larsson, A. Alijagic, O. Kotlyar, M. Engwall, V. Sjöberg, S. H. Keiter and R. Almeda, Cocktail Effects of Tire Wear Particles Leachates on Diverse Biological Models: A Multilevel Analysis, *J. Hazard. Mater.*, 2024, **471**, 134401, DOI: 10.1016/j.jhazmat.2024.134401.

26 A. J. Bergmann, T. Masset, F. Breider, W. Dudefoi, K. Schirmer, B. J. D. Ferrari and E. L. M. Vermeirssen, Estrogenic, Genotoxic, and Antibacterial Effects of Chemicals from Cryogenically Milled Tire Tread, *Environ. Toxicol. Chem.*, 2024, **43**(9), 1962–1972, DOI: 10.1002/etc.5934.

27 X. Hu, H. (Nina) Zhao, Z. Tian, K. T. Peter, M. C. Dodd and E. P. Kolodziej, Chemical Characteristics, Leaching, and Stability of the Ubiquitous Tire Rubber-Derived Toxicant 6PPD-Quinone, *Environ. Sci.: Processes Impacts*, 2023, **25**(5), 901–911, DOI: 10.1039/D3EM00047H.

28 K. L. Platt, O. Yushchenko, J. R. Laszakovits, Y. Zhang, N. C. Pflug and K. McNeill, Aquatic Thermal and Photochemical Reactivity of N-(1,3-Dimethylbutyl)-N′-Phenyl-p-Phenylenediamine (6PPD), N-Isopropyl-N′-Phenyl-p-Phenylenediamine (IPPD), and 6PPD-Quinone, *Environ. Sci. Technol.*, 2025, **59**(25), 12900–12909, DOI: 10.1021/acs.est.4c12896.

29 B. Seiwert, M. Nihemaiti, M. Troussier, S. Weyrauch and T. Reemtsma, Abiotic Oxidative Transformation of 6-PPD and 6-PPD Quinone from Tires and Occurrence of Their Products in Snow from Urban Roads and in Municipal Wastewater, *Water Res.*, 2022, **212**, 118122, DOI: 10.1016/j.watres.2022.118122.

30 K. Hiki, K. Asahina, K. Kato, T. Yamagishi, R. Omagari, Y. Iwasaki, H. Watanabe and H. Yamamoto, Acute Toxicity of a Tire Rubber-Derived Chemical, 6PPD Quinone, to Freshwater Fish and Crustacean Species, *Environ. Sci. Technol. Lett.*, 2021, **8**(9), 779–784, DOI: 10.1021/acs.estlett.1c00453.

31 Y. Zhou, L. Yixi, Q. Kong, J. Peng, Y. Pan, J. Qiu and X. Yang, Sunlight-Induced Transformation of Tire Rubber

Antioxidant N-(1,3-Dimethylbutyl)-N′-Phenyl-p-Phenylenediamine (6PPD) to 6PPD-Quinone in Water, *Environ. Sci. Technol. Lett.*, 2023, **10**(9), 798–803, DOI: 10.1021/acs.estlett.3c00499.

32 H. N. Zhao, X. Hu, Z. Tian, M. Gonzalez, C. A. Rideout, K. T. Peter, M. C. Dodd and E. P. Kolodziej, Transformation Products of Tire Rubber Antioxidant 6PPD in Heterogeneous Gas-Phase Ozonation: Identification and Environmental Occurrence, *Environ. Sci. Technol.*, 2023, **57**(14), 5621–5632, DOI: 10.1021/acs.est.2c08690.

33 Y. Xu, T. Wang, Z. Chen, Y. Li, D. Huang, F. Guo and M. Wang, Hydrolysis of P-Phenylenediamine Antioxidants: The Reaction Mechanism, Prediction Model, and Potential Impact on Aquatic Toxicity, *Environ. Sci. Technol.*, 2025, **59**(1), 811–822, DOI: 10.1021/acs.est.4c10227.

34 B. Liang, J. Li, B. Du, Z. Pan, L.-Y. Liu and L. E. Zeng, Waste Recycling Emits Large Quantities of Emerging Aromatic Amines and Organophosphites: A Poorly Recognized Source for Another Two Classes of Synthetic Antioxidants, *Environ. Sci. Technol. Lett.*, 2022, **9**(7), 625–631, DOI: 10.1021/acs.estlett.2c00366.

35 OSPAR Commission, *OSPAR Commission OSPAR Background Document on 4-(Dimethylbutylamino)Diphenylamine (6PPD)*, 2006.

36 R. A. Hites, Correcting for Censored Environmental Measurements, *Environ. Sci. Technol.*, 2019, **53**(19), 11059–11060, DOI: 10.1021/acs.est.9b05042.

37 M. A. Hoffmann, L.-F. Nothias, M. Ludwig, M. Fleischauer, E. C. Gentry, M. Witting, P. C. Dorrestein, K. Dührkop and S. Böcker, High-Confidence Structural Annotation of Metabolites Absent from Spectral Libraries, *Nat. Biotechnol.*, 2022, **40**(3), 411–421, DOI: 10.1038/s41587-021-01045-9.

38 K. Dührkop, M. Fleischauer, M. Ludwig, A. A. Aksenov, A. V. Melnik, M. Meusel, P. C. Dorrestein, J. Rousu and S. Böcker, SIRIUS 4: A Rapid Tool for Turning Tandem Mass Spectra into Metabolite Structure Information, *Nat. Methods*, 2019, **16**(4), 299–302, DOI: 10.1038/s41592-019-0344-8.

39 K. Dührkop, H. Shen, M. Meusel, J. Rousu and S. Böcker, Searching Molecular Structure Databases with Tandem Mass Spectra Using CSI:FingerID, *Proc. Natl. Acad. Sci. U. S. A.*, 2015, **112**(41), 12580–12585, DOI: 10.1073/pnas.1509788112.

40 C. Ruttkies, E. L. Schymanski, S. Wolf, J. Hollender and S. Neumann, MetFrag Relaunched: Incorporating Strategies beyond in Silico Fragmentation, *J. Cheminf.*, 2016, **8**(1), 3, DOI: 10.1186/s13321-016-0115-9.

41 A. Foscari, B. Seiwert, D. Zahn, M. Schmidt and T. Reemtsma, Leaching of Tire Particles and Simultaneous Biodegradation of Leachables, *Water Res.*, 2024, **253**, 121322, DOI: 10.1016/j.watres.2024.121322.

42 V. Kuntz, D. Zahn and T. Reemtsma, Quantification and Occurrence of 39 Tire-Related Chemicals in Urban and Rural Aerosol from Saxony, Germany, *Environ. Int.*, 2024, **194**, 109189, DOI: 10.1016/j.envint.2024.109189.

43 Z.-M. Li, V. K. Pal, P. Kannan, W. Li and K. Kannan, 1,3-Diphenylguanidine, Benzothiazole, Benzotriazole, and Their Derivatives in Soils Collected from Northeastern United States, *Sci. Total Environ.*, 2023, **887**, 164110, DOI: 10.1016/j.scitotenv.2023.164110.

44 R. B. Spies, B. D. Andresen and D. W. Rice Jr, Benzthiazoles in Estuarine Sediments as Indicators of Street Runoff, *Nature*, 1987, **327**(6124), 697–699, DOI: 10.1038/327697a0.

45 Q. Zhang, X. Wang, C. Liu, H. Li, Z. Deng, C. Yao, Y. Li, Q. Rao and W. Song, Accurate and Stable Detection of P-Phenylenediamine Antioxidants and Their Transformation Products in Aquatic Products Using Antioxidant Protection – Analysis of Actual Aquatic Products, *J. Hazard. Mater.*, 2024, **480**, 136099, DOI: 10.1016/j.jhazmat.2024.136099.

46 S. Pan, Y. Sun, G. Zhang, J. Li, Q. Xie and P. Chakraborty, Assessment of 2-(4-Morpholinyl) Benzothiazole (24MoBT) and N-Cyclohexyl-2-Benzothiazolamine (NCBA) as Traffic Tracers in Metropolitan Cities of China and India, *Atmos. Environ.*, 2012, **56**, 246–249, DOI: 10.1016/j.atmosenv.2012.03.029.

47 C. M. Reddy and J. G. Quinn, Environmental Chemistry of Benzothiazoles Derived from Rubber, *Environ. Sci. Technol.*, 1997, **31**(10), 2847–2853, DOI: 10.1021/es970078o.

48 M. H. McMinn, X. Hu, K. Poisson, P. Berger, P. Pimentel, X. Zhang, P. Ashara, E. L. Greenfield, J. Eig and Z. Tian, Emerging Investigator Series: In-Depth Chemical Profiling of Tire and Artificial Turf Crumb Rubber: Aging, Transformation Products, and Transport Pathways, *Environ. Sci.: Processes Impacts*, 2024, **26**(10), 1703–1715, DOI: 10.1039/D4EM00326H.

49 B. Seiwert, P. Klöckner, S. Wagner and T. Reemtsma, Source-Related Smart Suspect Screening in the Aqueous Environment: Search for Tire-Derived Persistent and Mobile Trace Organic Contaminants in Surface Waters, *Anal. Bioanal. Chem.*, 2020, **412**(20), 4909–4919, DOI: 10.1007/s00216-020-02653-1.

50 H. Kumata, Y. Sanada, H. Takada and T. Ueno, Historical Trends of N-Cyclohexyl-2-Benzothiazolamine, 2-(4-Morpholinyl)Benzothiazole, and Other Anthropogenic Contaminants in the Urban Reservoir Sediment Core, *Environ. Sci. Technol.*, 2000, **34**(2), 246–253, DOI: 10.1021/es990738k.

51 *NOCIL Limited Rubber Vulcanization*, https://www.scribd.com/document/283973137/Vulcanization-and-Accelerators, accessed July 2025.

52 E. L. Schymanski, J. Jeon, R. Gulde, K. Fenner, M. Ruff, H. P. Singer and J. Hollender, Identifying Small Molecules via High Resolution Mass Spectrometry: Communicating Confidence, *Environ. Sci. Technol.*, 2014, **48**(4), 2097–2098, DOI: 10.1021/es5002105.

53 I. Chipinda, J. M. Hettick, R. H. Simoyi and P. D. Siegel, Oxidation of 2-Mercaptobenzothiazole in Latex Gloves and Its Possible Haptenation Pathway, *Chem. Res. Toxicol.*, 2007, **20**(8), 1084–1092, DOI: 10.1021/tx700139g.

54 B. G. Brownlee, J. H. Carey, G. A. MacInnis and I. T. Pellizzari, Aquatic Environmental Chemistry of 2-(Thiocyanomethylthio)Benzothiazole and Related

Benzothiazoles, *Environ. Toxicol. Chem.*, 1992, **11**(8), 1153–1168, DOI: 10.1002/etc.5620110812.

55 H. Li, F. Han, L. Jiang, T. Yang, L. Du and J. Zhu, Continuous Synthesis of N-Cyclohexyl-2-Benzothiazole Sulfenamide with Microfluidics and Its Kinetic Study, *Ind. Eng. Chem. Res.*, 2021, **60**(39), 14134–14142, DOI: 10.1021/acs.iecr.1c02881.

56 R. Alhelou, B. Seiwert and T. Reemtsma, Hexamethoxymethylmelamine – A Precursor of Persistent and Mobile Contaminants in Municipal Wastewater and the Water Cycle, *Water Res.*, 2019, **165**, 114973, DOI: 10.1016/j.watres.2019.114973.

57 M. H. McMinn, Y. Tang, P. Berger, K. Poisson, A. Oliveira Tavares Lima, A. Stubbins, A. T. Güler and Z. Tian, From the Road to the Field: Decoding Chemical Transformation in Aging Tire and Artificial Turf Crumb Rubber, *Environ. Sci. Technol.*, 2026, **60**(1), 1051–1062, DOI: 10.1021/acs.est.5c08260.

58 T. Berger, J. Alenfelder, S. Steinmüller, D. Heimann, N. Gohain, D. Petras, M. Wang, R. Berger, E. Kostenis and R. Reher, A MassQL-Integrated Molecular Networking Approach for the Discovery and Substructure Annotation of Bioactive Cyclic Peptides, *J. Nat. Prod.*, 2024, **87**(4), 692–704, DOI: 10.1021/acs.jnatprod.3c00750.